Pharm Res (2012) 29:2601–2614
DOI 10.1007/s11095-012-0790-9

RESEARCH PAPER

Dextran-Catechin Conjugate: A Potential Treatment Against the Pancreatic Ductal Adenocarcinoma

Orazio Vittorio • Giuseppe Cirillo • Francesca Iemma • Giovanni Di Turi • Emanuela Jacchetti • Michele Curcio • Serena Barbuti • Niccola Funel • Ortensia Ilaria Parisi • Francesco Puoci • Nevio Picci

Received: 17 February 2012 / Accepted: 15 May 2012 / Published online: 24 May 2012

ABSTRACT

Purpose A polysaccharide-flavonoid conjugate was developend and proposed for the treatment of pancreatic ductal adenocarcinoma (PDAC).

Methods The conjugate was synthesized by free radical grafting reaction between catechin and dextran. The chemical characterization of the conjugate was obtained by UV-Vis, 1H-NMR, FT-IR and GPC analyses, while the functionalization degree was determined by the Folin-Ciocalteu assay. The biological activity of the catechin-dextran conjugate was tested on two different cell lines derived from human pancreatic cancer (MIA PaCa-2 and PL45 cells), and the toxicity towards human pancreatic nestin-expressing cells evaluated.

Results Both the cancer cell lines are killed when exposed to the conjugate, and undergo apoptosis after the incubation with catechin-dextran which resulted more effective in killing pancreatic tumor cells compared to the catechin alone. Moreover, our experimental data indicate that the conjugate was less cytotoxic to human pancreatic nestin-expressing cells which are considered a good model of non-neoplastic pancreatic cells.

Conclusion The suitability of newly synthesized Dextran-Catechin conjugate in the treatment of PDAC was proved confirming the high potential application of the proposed macromolecula system in the cancer therapy.

KEY WORDS anticancer activity · antioxidant-polymer conjugates · catechin · pancreatic ductal adenocarcinoma · polymeric drugs

INTRODUCTION

Pancreatic ductal adenocarcinoma (PDAC) is a lethal disease with a rising incidence such that it nowadays ranks as the fourth cause of cancer death in the Western world (1). Apart from cigarette smoking, which has been estimated to cause about 30% of pancreatic cancers (2), relatively little is known about the exact etiology of this disease, although other lifestyle factors have been implicated, including obesity (3) and type-II diabetes (4). Current therapy for PDAC is surgery followed by adjuvant radiotherapy and chemotherapy for early-stage and palliative chemotherapy for advanced disease (5) based on Gemcitabine as the standard cytotoxic agent (6,7). The variability of clinical response in PDAC patients is attributed to inter-individual differences in the pharmacokinetics and pharmacodynamics of gemcitabine as well as to the emergence of drug resistance and diminished sensitivity to radiotherapy (8). Recent studies have shown that gemcitabine therapy has a

O. Vittorio • E. Jacchetti
NEST Scuola Normale Superiore & Istituto Nanoscienze-CNR
Piazza San Silvestro
56126 Pisa, Italy

G. Cirillo (✉) • F. Iemma • O. I. Parisi • F. Puoci • N. Picci
Department of Pharmaceutical Sciences, University of Calabria
87036 Arcavacata di Rende (CS), Italy
e-mail: giuseppe.cirillo@unical.it

G. Cirillo • F. Iemma • O. I. Parisi • F. Puoci • N. Picci
Macrofarm Srl, University of Calabria
87036 Arcavacata di Rende (CS), Italy

G. Di Turi • N. Funel
Department of Oncology
Transplantation & Advanced Technologies in Medicine
University of Pisa
56100 Pisa, Italy

M. Curcio • S. Barbuti
Immunohematology Unit, Cisanello Hospital
56100 Pisa, Italy

beneficial effect on the quality of life of patients with PDAC treated with weekly infusions, although the median survival in these patients is only marginally prolonged (5). Regimens using combinations of gemcitabine with 5-FU with or without folinic acid, or combinations of gemcitabine with cisplatinum can prolong median survival for up to 8.3 months (9–11). The addition of radiation therapy to combination chemotherapy with mitomycin C and gemcitabine does not significantly improve survival (12). From the data previous showed, it is clear that there is a need for new more effective treatment against PDAC. This accounts for considerable research interest in newer cytotoxic agents and biological solutions for the treatment of PDAC, currently regarded as incurable in the vast majority of patients.

Among the different natural extract with improved biological properties, green tea is known to have a cancer chemopreventive effect against a broad spectrum of invasive solid cancers (13), with catechins (CT) as the key components responsible for these anti-proliferative properties. The major component in green tea extract, epigallocatechin-3-gallate (EGCG), has significant anti-tumorigenesis and anti-tumor growth effects (14). These effects of EGCG, and other structurally related green tea polyphenols, have been investigated using a variety of rodent tumor models. One of the most plausible mechanisms of their anti-proliferative activity is attributed to its ability to suppress the promotion of carcinogenesis in animals and in cultured cells, partially by the induction of apoptosis (15,16).

When studying the anticancer drugs, it should also be considered that most of them are small molecules, penetrating indiscriminately all cell types without any specific targeting, and this carries out to serious systemic toxicity. In the last few decades, to overcome these drawbacks by improving the targeted distribution of these drugs, thereby maximizing their anticancer effects with reduction of adverse effects on normal tissues, polymer-drug conjugates have been introduced (17). These drug delivery systems, functional materials in which the drug is covalently bonded to a polymeric carrier (18), carry out to several advantages (19) such as a passive tumor targeting by enhanced permeability and retention (EPR) (20); a decreased toxicity (21); an increased solubility in biological fluids (22); the possibility to overcome certain mechanisms of drug resistance and the ability to elicit immune-stimulatory effects (23). For the preparation of these conjugates, a variety of water-soluble polymers, e.g., human serum albumin and dextran, have been proposed. In all instances, the resulting drug-polymer conjugates have demonstrated good solubility in water, increased half-life in the body, and high antitumor effects (24).

In recent years, among the family of polymer conjugates, flavonoid-polymer conjugates have been proposed for biomedical applications (25) with the aim to increase the stability of the antioxidant molecule prolonging its duration of action (26). In particular, promising materials have been prepared through a free radical coupling between a preformed polymer (polysaccharide or protein) and a flavonoid in the presence of a water compatible redox pair such as hydrogen peroxide (H_2O_2) and ascorbic acid (AA). This approach has been successfully employed for the synthesis of chitosan, starch, inulin, alginate and gelatin derivatives with high antioxidant and biological properties, including anti-cancer activity (27).

In the present paper, for the first time, we report on the preparation of a catechin-dextran (CT-Dex) derivative with increased anticancer activity by comparing its antitumoral activity with that of free CT. Dextran (Dex) was selected as polymer because of its wide range of application in biomedical and pharmaceutical field. In particular, it is readily available, inexpensive, and it can be easily chemically modified. Furthermore, other properties such as high stability, hydrophilic and nontoxic nature and biodegradability render it an ideal drug delivery carrier (28). Regarding the cancer treatment, it was previously showed that dextran conjugation can increase the stability and the penetration in tumor mass of chemotherapeutic agents (29); moreover, a poly-L-arginine and dextran sulfate-based nano-sized polyelectrolyte complex was developed for the treatment of head and neck cancer (30).

In this work we tested the anti-tumor activity of the CT-Dex on two different cell lines derived from human pancreatic tumor, one of which was resistant to the standard chemotherapy agents. In particular, we studied the apoptosis induction by CT-Dex and its effects on the expression of VEGF gene, which is highly expressed in pancreatic tumor cells. Furthermore, its expression level correlates with microvessel density, tumor metastatic potential, local disease progression and chemo-resistance in a variety of malignancies, including PDAC (31,32).

MATERIALS AND METHODS

Synthesis of CT-Dex

The CT-Dex conjugate was synthesized according to the literature as follows (27): in a 50 mL glass tube, 0.5 g of Dex from *Leuconostoc* spp (Dex, Sigma, St. Louis, MO, USA) was dissolved in 50 mL distilled water. Then, 1 mL of H_2O_2 5.0 M (5.0 mmol) (Sigma, St. Louis, MO, USA) and 0.25 g of AA (1.4.mmol) (Sigma, St. Louis, MO, USA) was added and the mixture was maintained at 25°C under atmospheric air. After 2 h, in separate experiments, different amounts of CT, from 0.1 to 0.35 mmol, (Sigma, St. Louis, MO, USA) were introduced in the reaction flask and the mixtures were maintained at 25°C for 24 h under atmospheric air. The resultant polymer solutions were introduced into dialysis

tubes (of 6–27/32″ Medicell International LTD, MWCO: 3.5–5000 Da) and dipped into a glass vessel containing distilled water at 20°C for 48 h with eight changes of water. The resulting solutions were frozen and dried with a freeze drier (Micro Modulyo, Edwards Lifesciences, USA) to afford vaporous solids. Each purified conjugate was checked to be free of unreacted antioxidant and any other compounds by High-Pressure Liquid Chromatography (HPLC) analysis after the purification step. The HPLC analysis was carried out using a Jasco PU-2089 Plus liquid chromatography equipped with a Rheodyne 7725i injector (fitted with a 20 µl loop), a Jasco UV-2075 HPLC detector and Jasco-Borwin integrator (Jasco Europe s.r.l., Milan, Italy). A Tracer Excel 120 ODS-A column particle size 5 µm, 15×0.4 cm (Barcelona, Spain) was employed. As reported in literature (33), the mobile phase was a mixture of methanol/water/orthophosphoric acid (20/79.9/0.1) (HPLC grade, Carlo Erba, Milan, Italy) at a flow rate of 1.0 mL min^{-1}, while the detector was set at 260 nm.

Blank Dex, which acts as a control, was prepared when grafting process was carried out in the absence of CT.

Characterization of the Conjugate

Mn and Mw/Mn were measured by Gel permeation chromatography (GPC) using water as eluent at 25°C and at flow rate 1.0 mL min^{-1} on PL aquagel-OH Mixed, 7.5× 300 mm, 8 µm column in series with PL aquagel-OH 30, 7.5×300 mm, 8 µm (Agilent Technologies, Santa Clara CA USA) connected to a Jasco PU-2089 pump and a Jasco 930-RI refractive-index detector (Jasco Europe s.r.l., Milan, Italy). The columns were calibrated with standard Dextran samples (Sigma, St. Louis, MO, USA). IR spectra were recorded as KBr pellets on a Jasco FT-IR 4200 (Jasco Europe s.r.l., Milan, Italy). Spectrofluorimetric grade water (Sigma, St. Louis, MO, USA) was used for the photophysical investigations in solution, at room temperature. A Perkin Elmer Lambda 900 spectrophotometer (Perkin Elmer, Waltham, MA, USA) was employed to obtain the absorption spectra, while the corrected emission spectra, all confirmed by excitation ones, were recorded with a Perkin Elmer LS 50B spectrofluorimeter, equipped with Hamamatsu R928 photomultiplier tube. ^{1}H-NMR spectra were run on Bruker VM-300 ACP using DMSO-d6 as solvent.

Evaluation of CT Content by Folin-Ciocalteu Method

The amount of CT equivalents in the CT-Dex conjugate was determined using the Folin-Ciocalteu reagent procedure with some modifications (34). Briefly, 5 mg amount of CT-Dex conjugate was dispersed in distilled water (6 mL) in a volumetric flask. After dissolution, 1 mL of Folin-Ciocalteu reagent (Sigma, St. Louis, MO, USA) was added and the contents of flask were mixed thoroughly. After 3 min, 3 mL of Na_2CO_3 (2%) were added, and then the mixture was allowed to stand for 2 h with intermittent shaking. The absorbance was measured at 760 nm against a control prepared using the blank polymer under the same reaction conditions. The CT content in the conjugate was expressed as mg per g of dry conjugate by using the equation of the free CT calibration curve, recorded by employing five different CT standard solutions. 0.5 mL amount of each solution was added to the Folin-Ciocalteu system to raise the final concentration of 8.0, 16.0, 24.0, 32.0, and 40.0×10^{-6} mol L^{-1}, respectively. After 2 h, the absorbance of the solutions was measured to record the calibration curve and the correlation coefficient (R^2); slope and intercept of the regression equation obtained were calculated by the method of least squares.

Evaluation of the Antioxidant Properties

The antioxidant properties of CT-Dex conjugate were evaluated by determination of the scavenging activity towards DPPH, ABTS, hydroxyl and peroxyl radicals. All the tests were performed on CT-Dex conjugate, blank Dex to evaluate the interference of the polymeric material on the assay and free CT to determine the IC_{50} values of the free antioxidant (25–27).

For the DPPH assay, in five different test tubes, different amount of CT-Dex comjugate (1.0; 2.0; 3.0; 4.0; 5.0 mg) were dispersed in 10 mL of a DPPH solution in ethanol (100×10^{-6} mol L^{-1}, Sigma, St. Louis, MO, USA). The tubes were incubated in a water bath at 25°C and, after 30 min, the residual DPPH concentration was determined colorimetrically at 517 nm. The decrease (%) in DPPH absorbance was used to calculate the IC_{50} according to the following equation 1:

$$inhibition(\%) = \frac{A_0 - A_1}{A_0} \times 100 \quad (1)$$

where A_0 is the absorbance of a standard prepared in the same conditions, but without any polymers, and A_1 is the absorbance of polymeric samples.

The ABTS assay was performed as follows: ABTS radical cation was generated by incubation of ABTS (7.0×10^{-3} mol L^{-1}, Sigma, St. Louis, MO, USA) and potassium persulfate (2.45×10^{-3} mol L^{-1}, Sigma, St. Louis, MO, USA) in the dark at room temperature for 16 h. The solution was further diluted with ethanol to an absorbance of 0.70±0.02 measured at 734 nm and equilibrated at 30° C. Polymeric samples (10; 20; 30; 40; 50 µg) were added to 2.0 mL of ABTS radical cation solution and the absorbance at 734 nm was recorded 6 min after mixing. The IC_{50} value was calculated according to the equation 1.

The scavenging effect on hydroxyl radical was evaluated by studying the competition between the CT-Dex conjugate and the deoxyribose for hydroxyl radical formed by H_2O_2/Fe/ascorbate system using the Fenton reaction. Differen amounts of CT-Dex (1.0; 1.5; 2.0; 2.5; 3.0 mg) were dispersed in 0.5 mL of 95% ethanol and incubated with 0.5 mL deoxyribose (3.75×10^{-3} mol L^{-1}, Sigma, St. Louis, MO, USA), 0.5 mL H_2O_2 (1.0×10^{-3} mol L^{-1}, Sigma, St. Louis, MO, USA), 0.5 mL $FeCl_3$(100×10^{-3} mol L^{-1}, Sigma, St. Louis, MO, USA), 0.5 mL EDTA (100×10^{-3} mol L^{-1}, Sigma, St. Louis, MO, USA) and 0.5 mL ascorbic acid (100×10^{-3} mol L^{-1}, Sigma, St. Louis, MO, USA) in 2.0 mL potassium phosphate buffer (20×10^{-3} mol L^{-1}, pH 7.4, Sigma, St. Louis, MO, USA) for 60 min at 37°C. Then samples were filtered and to 1 mL amount of filtrate were added to 1 mL of thiobarbituric acid (1% *w*/*v*, Sigma, St. Louis, MO, USA) and 1 mL of trichloroacetic acid (2% *w*/*v*, Sigma, St. Louis, MO, USA) were added, and the mixtures were incubated at 100°C for 20 min. After cooling, the absorbance of the mixture was read at 535 nm against reagent blank. The antioxidant activity was expressed as a percentage of scavenging activity on hydroxyl radical according to equation (1).

The inhibition of lipid peroxidation was evaluated by performing the linoleic acid β-carotene test. In this assay, 1.0 mL of β-carotene solution (0.2 mg/mL in chloroform, Sigma, St. Louis, MO, USA) was added to 0.02 mL of linoleic acid (Sigma, St. Louis, MO, USA) and 0.2 mL of Tween 20 (Sigma, St. Louis, MO, USA) and then the chloroform was removed in a rotary evaporator. After evaporation, 100 mL of distilled water was added slowly to the mixture and agitated vigorously to form an emulsion. The emulsion (5.0 mL) was transferred to different test tubes containing different amounts of CT-Dex conjugate (5.0; 10.0; 15.0; 20.0; 25.0 mg). The tubes were then gently shaken and placed in a water bath at 45°C for 60 min. The absorbance of the filtered samples and control was measured at 470 nm against a blank, consisting of an emulsion without β-carotene. The measurement was carried out at the initial time (t=0) and successively at 60 min. Data are expressed as inhibition (%) according to the following equation (2):

$$A_{ox}A = \left(1 - \frac{A_0 - A_{60}}{A_0^o - A_{60}^o}\right) \quad (2)$$

where A_0 and $A_0°$ are the absorbance values measured at the initial incubation time for samples and control, respectively, while A_{60} and $A_{60}°$ are the absorbance values measured in the samples and in control, respectively, at t=60 min.

Freeze–Thaw Stability

Tubes containing free CT and CT-Dex conjugate (1.0×10^{-6} mol referred to CT) were kept at 2–8°C for 2 days, and then heated at 40°C for 2 days per cycle; three cycles of freeze-thaw were conducted (35). After this time, 10 mL of water were added to the samples and the solutions were analyzed by Folin Ciocalteu method. The freeze–thaw stability was evaluated by comparing the results after each cycle to the CT calibration curve.

Cell Culture

The human pancreatic cancer cell line (MIA PaCa-2) and the pancreatic ductal adenocarcinoma cell line (PL45) were obtained from American Type Culture Collection (ATCC, Rockville, MD). These cell lines were grown in a complete culture medium consisting of DMEM (Lonza, Milan, Italy) supplemented with 2 mM L-glutamine, 100 IU mL^{-1} penicillin, 100 μg mL^{-1} streptomycin and 10% heat inactivated fetal bovine serum (FBS, Lonza, Milan, Italy).

The human pancreatic Nestin-expressing cells (HPNE) generously provided by Prof. Daniela Campani (University of Pisa) were used as a control cell line. These cells were derived from non-neoplastic pancreatic tissue and immortalized using hTERT (36). We maintained HPNE in DMEM high glucose supplemented with 2 mM L-glutamine, 100 IU mL^{-1} penicillin, 100 μg mL^{-1} streptomycin, 10 ng mL^{-1} human recombinant EGF. Moreover, in the starving medium we added 2.5% of inactivated FBS and in the complete culture medium (for proliferating cells) we used 10% of inactivated FBS. Cells were maintained at 37°C in a saturated humidity atmosphere of 95% air and 5% CO_2.

In Vitro Studies for Evaluation of Cytotoxic Activity of CT and CT-Dex

Pancreatic cancer cell lines were chosen as an *in vitro* model system to test the cytotoxicity of CT and CT-Dex at different concentration (referred to CT concentration). Cells were grown in T75 cm^2 or T25 cm^2 tissue culture flasks (Costar, Cambridge, MA, USA), in an atmosphere of 5% CO_2 at 37°C, and were detached with a solution of trypsin-EDTA when they were in logarithmic phase of growth.

Trypan Blue Assay

Cell viability was assayed using a trypan blue exclusion test with slight modifications (37). We used this assay to find the concentration of CT-Dex complex with the best antitumor activity in the MIA PaCa-2 and PL45 cell lines. The tripan blue assay was also used as double check of the results obtained in the other assays and to identify the IC_{50} of CT and CT-Dex in pancreatic tumor cell and on HPNE cell monitored for 12 h after the treatment.

MTT Cell Proliferation Assay

Cytotoxicity was also assessed by 3-(4,5-dimethylthiazole-2-yl)-2,5-diphenyl tetrazolium bromide, (MTT, Sigma, St. Louis, MO, USA), In this assay, the mitochondrial dehydrogenase of viable cells reduces the water-soluble MTT to water-insoluble formazan crystals. The MTT-containing medium is then replaced with 100 μL of DMSO (Sigma St. Louis, MO, USA) and left for 10 min on a platform shaker to solubilize the converted formazan. The absorbance is measured on a Versamax microplate reader (Molecular Devices, Sunnyvale, CA, USA) at a wavelength of 570 nm with background subtracted at 690 nm. Cells were seeded in 96-well sterile plastic plates (Costar, Cambridge, MA) at 25×10^3 cells/100 μL into each well and allowed to attach for 6 h. Firstly, we performed the MTT after the incubation for 12 h with 100 μg mL^{-1}, 150 μg mL^{-1}, 200 μg mL^{-1}, 300 μg mL^{-1}, 500 μg mL^{-1}, 800 μg mL^{-1} and 1200 μg mL^{-1} of CT and CT-Dex to calculate the IC_{50}. Starting from the data obtained by the trypan blue and the MTT assays for the IC_{50} calculation, we decided to investigate the effect of time of incubation of two concentrations of CT and CT-Dex (150 μg mL^{-1} and 300 μg mL^{-1}). Cells were then treated with 6 different media: 1) complete DMEM (control); 2) DMEM supplemented with Dex; 3) DMEM supplemented with CT 150 μg mL^{-1}; 4) DMEM supplemented with CT 300 μg mL^{-1}; 5) DMEM supplemented with CT-Dex 150 μg mL^{-1}; 6) DMEM supplemented with CT-Dex 300 μg mL^{-1}. We performed the MTT assays at three different time of incubation: 24 h, 48 h and 72 h. Cell growth inhibition will be expressed as percentage of live cells in control cultures and the % of live cells in treated cultures.

Effect of CT and CT-Dex on Non-Neoplastic Cells

We used the HPNE cells as model to compare the different effect of the CT and CT-Dex on non-neoplastic and tumour cells. In these experiments we starved HPNE cells by incubating them with culture medium with 2% of FBS, 16 h before to add the CT and CT-Dex. When cells are starved they do not proliferate and remain in G0 phase of the cell cycle similar to the primary cells. MTT and trypan blue assay were performed as previous described, to investigate if drugs have an effect only on highly proliferative cell without compromising the viability of non-neoplastic pancreatic cells.

Oxidative Stress

CT is generally well known as an antioxidant; however in certain conditions it can induce reactive oxidative stress species (ROS) in tumor cells (38). In order to study the ROS production in cells treated with CT and CT-Dex was detected by using the Image-IT Green Reactive Oxygen Species Detection kit (Invitrogen, Milan, Itay). The assay is based on 5-(and-6)-carboxy-2′,7′-dichlorodihydrofluorescein diacetate (carboxy-H_2DCFDA), a fluorogenic marker for ROS in viable cells. Tert-butyl hydroperoxide (TBHP, Invitrogen, Milan, Italy) was used as a positive control because it is a known inducer of ROS production (39). We studied the ROS production in cells after 30 min of incubation with CT and CT-Dex by following manufacturer's instructions. We examined the cells by Nikon's epi-fluorescence microscopy (Nikon, TE2000 model) using a filter set for FITC. The number of positive ROS green cells was counted on five randomly selected areas from three cover slips from each experimental group. Results are expressed as percentage of ROS positive cells of the total number of cells.

Annexin V Staining for Evaluation of Apoptotic Cell Death

Annexin V was used as a probe to detect cells that have expressed phosphatidylserine on the cell surface, a feature found in apoptosis cell death. 20×10^4 cells cultured on cover slips were exposed for 30 min to modified culture media as previously described; control cells were incubated with complete culture medium. MIA PaCa-2 and PL45 cell death was evaluated by the ApoAlert Annexin V assay (Clontech-Takara Bio Europe, Saint-Germain-en-Laye, France), to detect apoptosis at a very early stage, following the instruction of ApoAlert® Annexin V User Manual. In addition, we co-stained the cells with blue fluorescent with 0.5 μg mL^{-1} Hoechst 33258 (Sigma, St. Louis, MO, USA) to distinguish blue nucleus from green annexin V on the cell membrane. Finally, we examined the cells by Nikon's epi-fluorescence microscopy (Nikon, TE2000 model) using a dual filter set for FITC & DAPI. The number of annexin V green cells was counted on five randomly selected areas from three cover slips from each experimental group. Results are expressed as number of apoptotic cells as a percentage of the total number of cells and compared to the control sample.

RT-PCR Characterization of mRNA Expression of VEGF Gene in Pancreatic Tumor Cell Lines

The RNA from pancreatic cancer cells was extracted using the QiaAmp RNA mini-Kit (Qiagen, San Diego, CA), according to the manufacturer's instructions. Genomic DNA was removed by a DNase treatment with RNase-free DNase set (Qiagen, San Diego, CA). The amount of extracted RNA was quantified by measuring the absorbance at 260 nm. The purity of the RNA was checked by measuring the ratio of the absorbance at 260 and 280 nm, where a ratio ranging from 1.8–2.0 was regarded as pure. The absence of degradation of the RNA was confirmed by RNA electrophoresis on a 1.5%

agarose gel containing ethidium bromide. Total RNA (0.5 μg) was reverse-transcribed into cDNA by using VersoTM cDNA Kit (Thermo Fisher Scientific, Milan, Italy) according to the manufacturer's instructions. RT product was aliquoted in equal volumes and stored at −20°C. The conditions for the reverse transcription were incubation at 50°C for 30 min, followed by inactivation at 85°C for 5 min.

Real-time quantitative RT-PCR (qRT-PCR) was performed by using the SYBR Green Master Mix technique, according to the manufacturer's instructions. The reactions were prepared in a total volume of 25 μL containing: 5 μL volume cDNA, 1 μL of each primer (forward and reverse 10 μM), 12.5 μL of SYBR Green master mix, and 5.5 μL of sterile water. All samples were run in triplicate on 96-well reaction plates with the iQ™5 Multicolor Real-Time PCR Detection System©. The real-time amplification conditions included 3 min at 95°C, followed by 40 cycles at 96°C for 30 s and at 56°C for 1 min. Baseline and threshold values were automatically determined for all plates using the Bio-Rad iQ5 Software 2.0. PCR efficiencies were calculated from a standard curve, derived from a five cDNA dilution series in triplicate and gave regression coefficients greater than 0.98 and efficiencies greater than 96%. The standard curves were obtained using the GAPDH and VEGF gene primers, amplified with 1.6, 8, 40, 200 and 1000 μg μL^{-1} of total cDNA. Gene expression variation was calculated for individual reference genes based on cycle threshold (Ct) values, correlation coefficient (R2), real-time PCR efficiencies (E) and slope values, generated of each standard curve. The curves obtained for each cell line showed a linear relationship between RNA concentration and the Ct value of PCR real time for all genes. Real-time was calculated from the given slopes in the iQ Real Time PCR System software according to the equation: $(E = 10 - (1/b) - 1$; where b = regression coefficient).

All the amplifications were carried out with normalization of gene expression against the glyceraldehyde 3-phosphate dehydrogenase (GAPDH) reference gene. Estimation of gene expression was calculated according to the 2-ΔΔCt method (Table I shows the primers used in the Real Time PCR).

Statistical Analysis

Each experiment was carried out in triplicate. For the antioxidant experiments, data are expressed as means (±SD). For the calculation of the fluorescence assays, five random microscopic fields per cover slip were counted and three cover slips/ treatment were used for each test. Statistical significance was assessed by one way analysis of variance (ANOVA) followed by post-hoc comparison test (Tukey). Significance was set at 5%.

RESULTS AND DISCUSSION

Synthesis and Characterization of CT-Dex Conjugate

The synthesis of CT-Dex was performed by free radical reaction induced by H_2O_2/AA redox pair. As reported elsewhere, this synthetic strategy allows functionalizing natural polymers with bioactive molecules without the generation of toxic by-products and without using any kind of chemical reactant or organic solvent (26). We used only water, hydrogen peroxide and ascorbic acid for the covalent insertion of CT into the polymeric chain of Dex. The reaction mechanism involves a complex radical reaction between Dextran and Catechin. In particular, the interaction between the redox initiator pair (H_2O_2 and ascorbic acid) carries out to the formation of hydroxyl radicals attacking the hydrogen atoms on dextran in the α-methylene (CH_2) position and hydroxyl position (OH) of dextran (26). The subsequent linkage of the CT molecules involves reaction with these reactive sites. The possibility to obtain a radical coupling of phenolic compounds is proved in literature (40), and involves the reaction between the ortho- and para- positions relative to the hydroxyl group of the flavonoid and the heteroatoms of the biomacromolecule (27).

To maximize the functionalization of Dex with CT, the optimization of the reaction conditions was performed by varying the amount of CT from 0.1 to 0.35 mmol (the highest amount of CT which can be dissolved in the reaction feed). Each of the resulting polymer-antioxidant conjugates was purified and characterized by Folin-Ciocalteu method to determine the functionalization degree. The most performing material was obtained when 0.35 mmol of CT were used: a lower amount of CT, indeed, carried out to materials with lower antioxidant properties.

The absence of free CT in the sample was confirmed by checking the absence of peak at the retention time of CT in the HPLC analysis of the washing media employed in the dialyses process. HPLC and ^{1}H-NMR analyses were used to

Table I Primers used in the Real Time PCR

PRIMERS forward and reverse	
VEGF	
CGAAACCATGAACTTTCTGC	CCTCAGTGGGCACACACTCC
GAPDH	
CTCAAGATCATCAGCAATGCCTCCT	TTGGTATCGTGYAAGGACTCATGACC

assess that the reaction condition did not affect the CT structure. After the dialysis process, indeed, the residual CT in the washing media were analysed and no differences in the CT retention time and in the peak resolution were indeed detected by HPLC, as well as no changes in the 1H-NMR spectra were recorded.

Indications of the covalent modification of Dex with CT were obtained by UV-Vis, ^{1}H-NMR and FT-IR analyses.

As previously reported (25–27), the covalent insertion of a flavonoid into a polymeric chain is highlighted by a bathochromic shift of the UV-Vis absorption and emission peaks related to the aromatic region of the antioxidant. By virtue of the linkage with the hetero-atoms of Dex, an extension of the conjugation of the CT aromatic part occurs with a shift of the absorption peaks from 207 and 230 nm to 241 and 286 nm (moving from free to conjugated form) and of the emission peak from 319 to 411 nm (Fig. 1). Blank Dex showed no peaks in the aromatic region.

In Fig. 2, the ^{1}H-NMR spectra of CT (a), Dex (b) and CT-Dex (c) are reported. By comparing these spectra, the presence of the antioxidant in the polymeric backbone is confirmed. In the CT spectra, aromatic and phenolic ^{1}H can be recorded at 6.6–6.9 and 8.8–9.2 ppm respectively, while the blank Dex shows no signals in this range typical of aromatic systems. In the conjugate, broad signals at 6.4–6.7 related to aromatic ^{1}H and at 8.6–9.0 ppm related to phenolic ^{1}H are detected. The wide chemical shift range in the aromatic and phenolic ^{1}H of CT-Dex are related to the grafting reaction, which randomly involves the phenolic groups of the flavonoid as well as the position 6 and 8 of CT A ring and 2′ and 5′ of CT B ring (Fig. 2) as reported in literature (25).

The FT-IR spectra analyses of Dex, CT-Dex and CT confirmed the appearance of the carbon to carbon stretching band within the aromatic ring in the conjugate (Fig. 1).

To assess that the reaction conditions did not affect the Dex structure, GPC analysis was performed to determine the average molecular weight of native and conjugated Dex. The results showed an average molecular weight of 4000 Da (M_w/M_n<2.5) of Dex which is almost unchanged in CT-Dex (4000 Da with M_w/M_n<2.6).

A key characterization of the conjugate is the determination of the amount of CT into the polymeric backbone. This was performed by using the Folin-Ciocalteu assay, which determines the efficiency of the antioxidant residues in reducing a molybdenum complex within the Folin-Ciocalteu reagent (34). Specifically, the amount of CT into the conjugate was determined by comparison of the reducing power

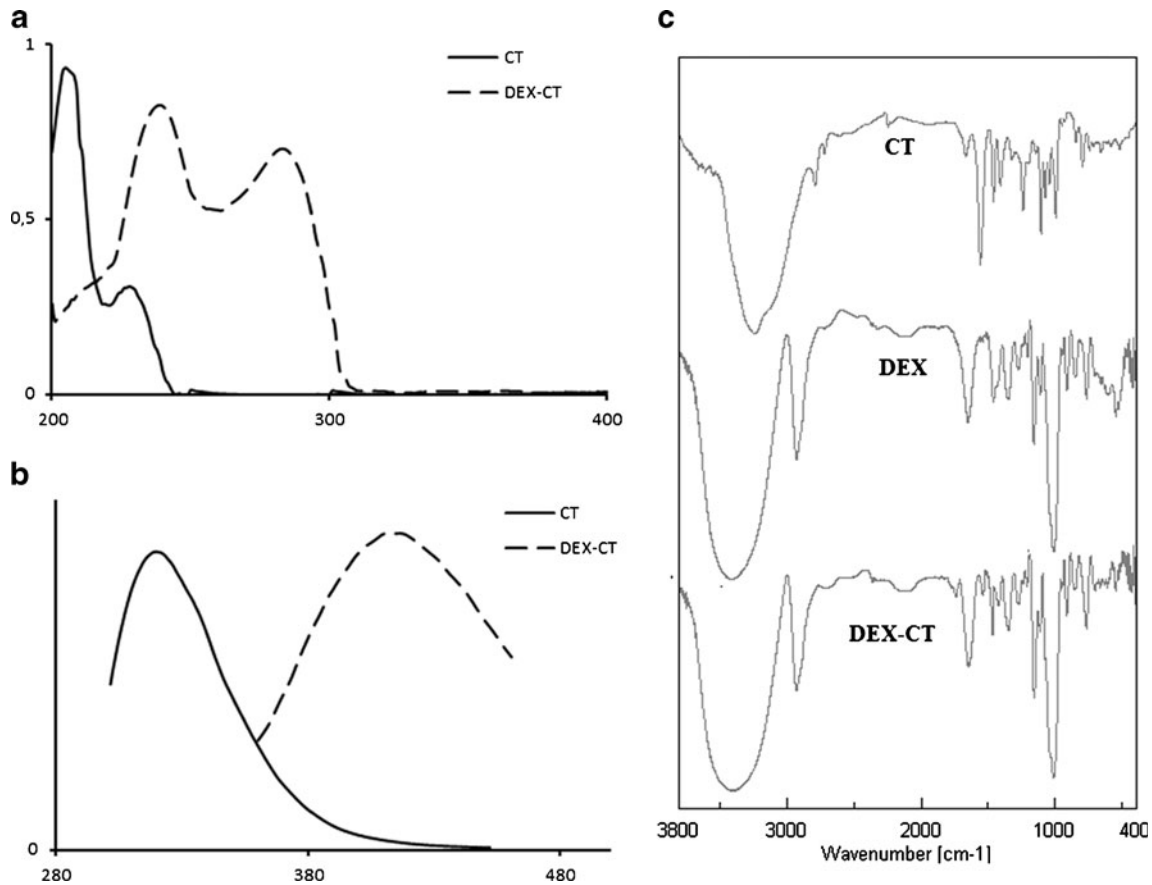

Fig. 1 (**a**) UV-Vis spe ctra: CT (—), CT-Dex (- -); (**b**) Emission spectra CT (—), CT-Dex (- -), (**c**) FT-IR spectra of CT, Dex and CT-Dex.

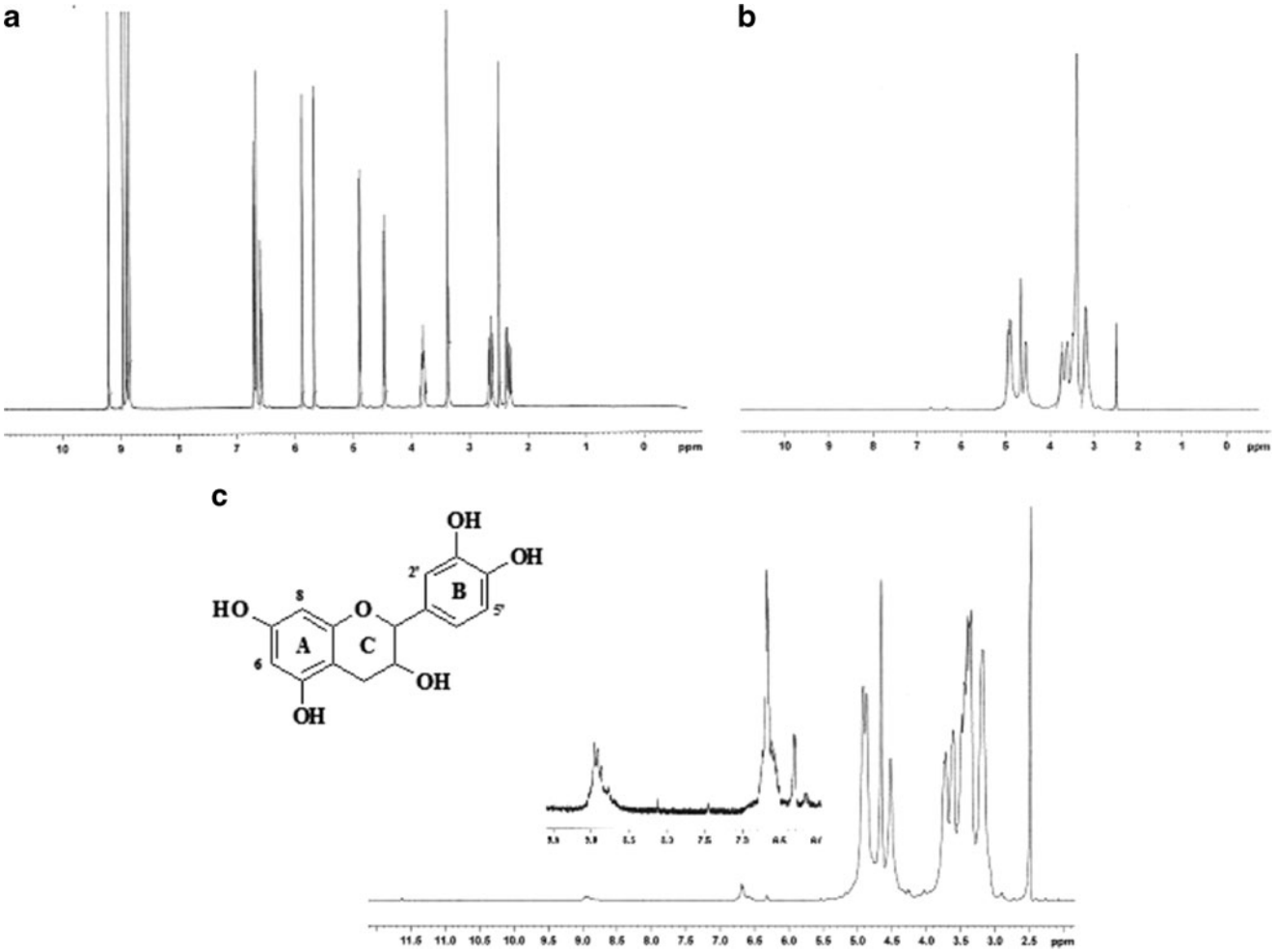

Fig. 2 ^{1}H-NMR spectra of CT (**a**), DEX (**b**) and DEX-CT (**c**).

of CT and CT-Dex to form the spectrophotometrically detectable blue species $(PMoW_{11}O_{40})^{4-}$. As a result, 1.0 g of polymer contains 19.9 ± 0.6 mg of CT. To assess that the reducing power of CT was not significantly affected by the conjugation process with Dex, four different tests measuring the CT antioxidant efficiency were performed and the recorded IC_{50} values obtained for CT-Dex were compared with those of the free antioxidant. In particular, the reducing power towards two stable free radicals, the hydrophobic DPPH and the hydrophilic ABTS radical, were determined, and the IC_{50} values collected in Table II and, by considering the functionalization degree obtained by the Folin-Ciocalteu assay (19.9 mg of CT per g of conjugate), also expressed as CT equivalent concentrations. These values were found to be very similar to the IC_{50} of free CT, confirming that the conjugation process did not interfere with the CT properties and the suitability of calculating the functionalization degree by means of the determination of the reducing power by Folin-Ciocalteu method.

In addition, the ability of the CT-Dex conjugate in inhibition the free radical formation was evaluated. The deoxyribose and linoleic systems were used as source of hydroxyl and peroxyl radicals, respectively, and the results confirmed that CT-Dex was able to inhibit the formation of these radicals with efficiency comparable to those of free CT. In all the antioxidant experiments, the interference of Dex was very low (below 2%).

Finally, the increased stability of CT in the conjugate with respect to the free form was assessed by Freeze–thaw

Table II Antioxidant Properties of Free CT and CT-Dex Conjugate (Expressed as Polymer Concentration and CT Equivalent Concentration)

Free radical	IC_{50}		
	CT	CT-Dex	
	μM	mg/ml	CT equivalents (μM)
DPPH	19.0 ± 0.4	0.28 ± 0.2	19.9 ± 0.5
ABTS	1.16 ± 0.5	0.02 ± 0.1	1.37 ± 0.4
Hydroxyl	25.3 ± 1.4	0.38 ± 0.3	26.1 ± 0.5
Peroxyl	254.1 ± 1.5	3.89 ± 1.1	266.9 ± 1.3

stability test. After three temperature cycles, the antioxidant power of free CT was reduced by 77.0±1.4%, while only a 4.1±1.6% of reduction was recorded for CT-Dex, confirming our hypothesis that the conjugation to a macromolecular system significantly increases CT stability, leading to a sustained activity of the flavonoid.

Evaluation of the Anticancer Activity

In our study we investigated the effectiveness of the CT-Dex to kill pancreatic tumor cells. We used the trypan blue exclusion test and the MTT assay for the estimation of the IC_{50} of the new conjugate CT-Dex on pancreatic tumour cells after the incubation for 12 h with 50 μg mL^{-1}, 100 μg mL^{-1}, 150 μg mL^{-1}, 200 μg mL^{-1} and 300 μg mL^{-1} of CT-Dex. Moreover we investigated the IC_{50} of this conjugate on starved HPNE cells, which represent a good model to study the possible side effects on non-neoplastic pancreatic cells. HPNE are not tumor cells, however they are immortalized cells lines and, in order to mimic the non neoplastic behavior, we starved these cells by incubating them with culture medium with 2.5% of serum. In a different experiment, cells were incubated with 10% of serum in order to make them grow and duplicate like cancer cells do; the high proliferation rate is, indeed, indicative of the neoplastic progression (41).

The data showed that CT-Dex has an IC_{50} of 838.33 μg mL^{-1} on the starved HPNE incubated with 2.5% serum and 416 μg mL^{-1} on the HPNE incubated with 10% serum, 377.7 μg mL^{-1} on the MIA PaCa-2 and 295.34 μg mL^{-1} on the PL45. We also calculated the IC_{50} of CT on MIA PaCa-2 and PL45 cells and the values were 1.197 mg mL^{-1} and 1.032 mg mL^{-1} respectively. Moreover we did not observe any negative effect in starved HPNE incubated for 12 h at all the tested concentrations of CT.

Our experiments showed that catechin-dextran conjugate had different IC_{50} values for pancreatic tumour cells and for starved HPNE, suggesting that the activity of our drug strongly depends on the cells proliferation rate and metabolism. Even if we cannot claim the cancer-cell-selective cytotoxicity of the conjugate, our results underline an increased susceptibility of high proliferative cells at the dextran-catechin. Furthermore, these results are interesting because they confirm the increased antitumor activity of the CT-Dex on pancreatic cancer cell compared with the free CT.

The MTT assay was used to detect the viability of cells by measuring the formation of a formazan product as an index of the cellular mitochondrial dehydrogenase activity. After obtaining the IC_{50} results, we decided to study the effect of CT and CT-Dex at two different concentrations 150 μg mL^{-1} and 300 μg mL^{-1} after long time of exposure: 24 h, 48 h and 72 h of continuous incubation. As shown in Fig. 3, data obtained with the MTT test indicated about 97% loss of viability after 72 h of incubation with CT-Dex at 150 μg mL^{-1} and 300 μg mL^{-1} in both pancreatic tumour cell lines. Furthermore, in the PL45, which are usually refractory at the treatment with gemcitabine and other cytotoxic agents, CT-Dex killed the 80% of cells after 24 h of incubation (Fig. 4), whereas we have the same effect on MIA PaCa-2 after 48 h of incubation. The time dependent MTT results showed that CT-Dex conjugate is more effective in cells with a high metabolism such us the PL45.

The increased anticancer activity of CT-Dex conjugate in comparison with the free flavonoid is related to both chemical and biological effects. The chemical effect is an increase in the CT stability after conjugation, as showed by the specific stability tests. In order to evaluate the biological component, we performed additional experiments in which the pancreatic tumor cell lines were incubated with a fluorescent dextran and, as a result, we observed that dextran was fast internalized by the cells. In particular, the FITC-dextran was observed inside the cells after 20 min of incubation (data not shown but available from the authors), and according to several literature data, we suggest that Dex improves the CT transport inside the cells by macropinocytosis process (42).

Regarding the molecular mechanism of the cytotoxicity, there are some reports in the literature showing that CT can induce many damages in cancer cell leading to their apoptosis: oxidative stress, depolarization of mitochondrial membrane, release of cytochrome P450, downregolation of transcripition factors (13–15). We investigated the possibility of CT-Dex to induce reactive oxygen species and apoptosis. In Fig. 5 we showed the studies about the ROS generation in cells after treatment with CT and CT-Dex. Our results clearly showed that CT-Dex is more active in inducing oxidative stress at both concentration (150 and 300 μg mL^{-1}) and in both tumour cells. The level of ROS production in cells treated with the conjugate was significantly higher in comparison with free CT at the same concentration. Because the ROS induction can lead cells towards an apoptotic fate, we performed the labeled annexin V to detect the cells in early stage of apoptosis after their incubation for 30 min with CT and CT-Dex. As it is shown in the Fig. 6 MIA PaCa-2 cells showed 62% of annexin positive cells after 30 min of incubation with CT-Dex 150 μg/ml, whereas it was observed a 73% of positive cells with 300 μg mL^{-1} of the conjugate. Moreover, PL45 tumour cells counted 67% of positive cells with CT-Dex 150 μg mL^{-1} and 85% of green positive cells with CT-Dex 300 μg mL^{-1}. These results are in accordance with the studies about the ROS generation in cells incubated with CT-Dex. To confirm that our new CT-Dex conjugate can represent a good candidate for the treatment of PDAC, we performed real time PCR to study the expression level of the

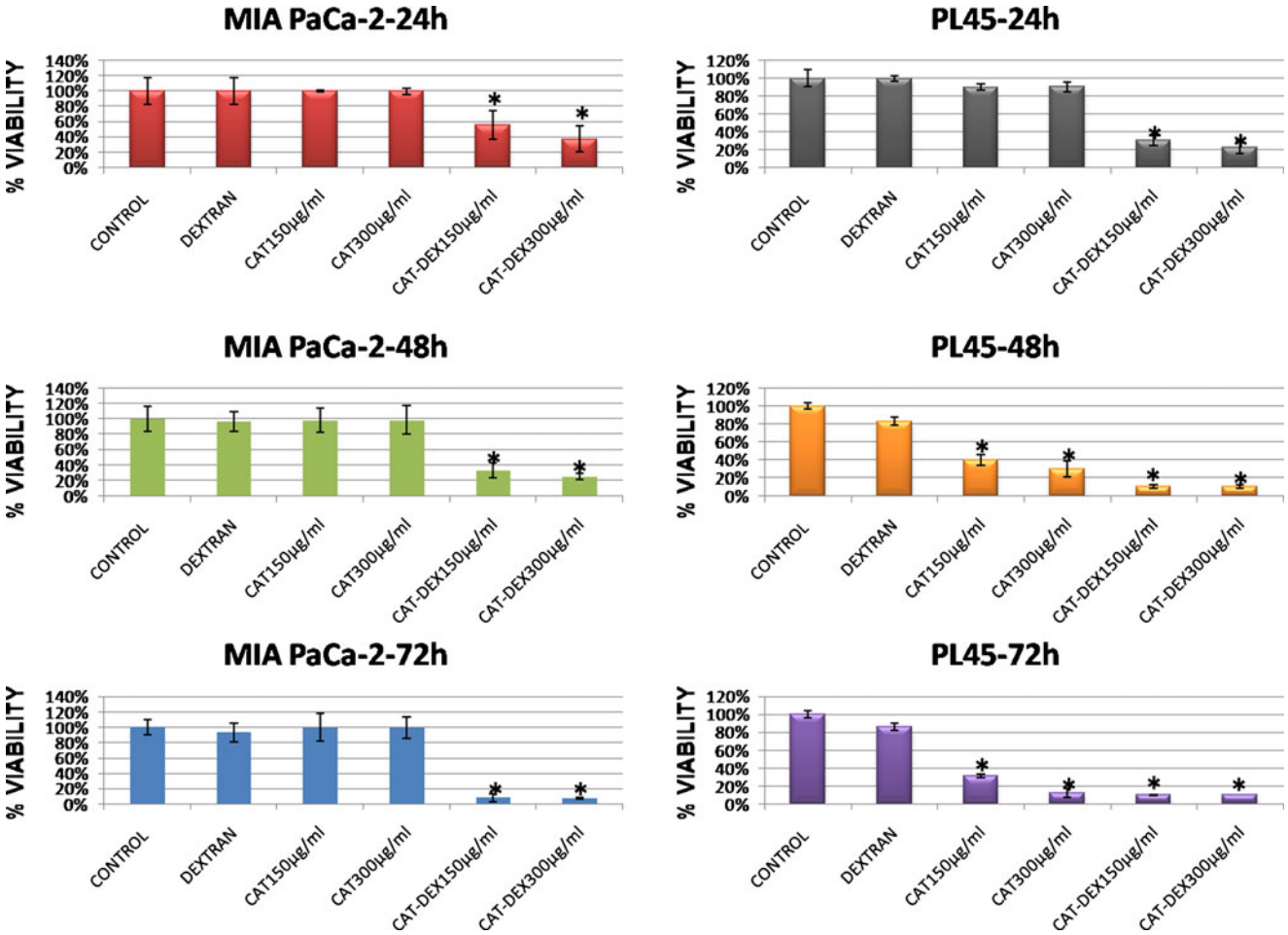

Fig. 3 Histograms of cell proliferation (MTT) of MIA PaCa-2 and PL45 cells after 24 h, 48 h and 72 h of incubation with dextran, catechin and dextran-catechin conjugate at 150 μg/ml and 300 μg/ml. An increased loss of viability was observed in cells treated with dextran-catechin conjugate compared with the catechin alone. Results are expressed as means ± S.E.M.(vertical bars) of three experiments each carried out in sixplicate. (* $P < 0.05$ in comparison with controls).

vascular endothelial growth factor (VEGF). It is well known that VEGF is an over expressed gene, involved in the new vessels formation in the tumour mass and its high expression level often correlates with tumor metastatic potential, local disease progression and chemo-resistance in a variety of malignancies, including PDAC (32). We performed the real

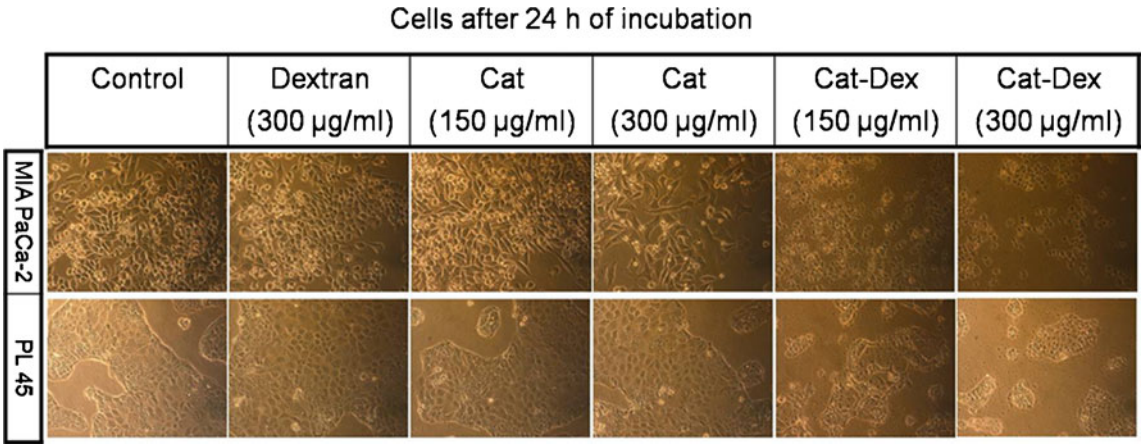

Fig. 4 Bright field pictures of MIA PaCa-2 and PL45 cells after 24 h of continuous incubation with dextran, catechin and dextran-catechin conjugate. In the picture of both tumor cell lines there is a strong effect of the dextran-catechin conjugate at both tested concentration. There are many died cells in the samples trated with the dextran-catechin conjugate. In sharp contrast, the catechin alone at the same concentration was harmless on the tumor cells.

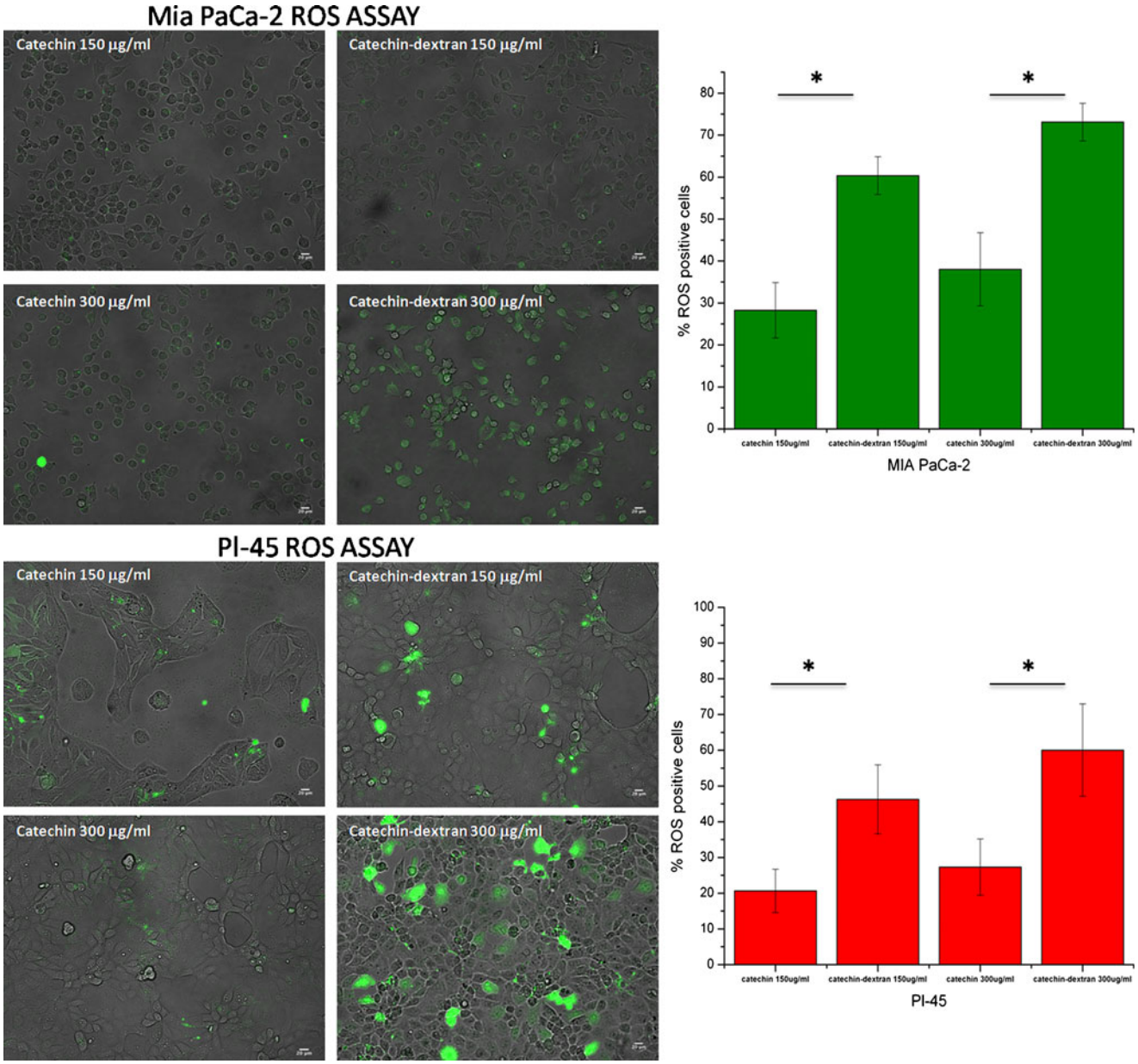

Fig. 5 Detection of intracellular ROS in Mia PaCa-2 and PL45 cells treated with catechin and catechin-dextran at 150 μg/ml and 300 μg/ml. We represented the percentage of ROS positive cells in the plots. (* $P < 0.05$ $n=3$).

time PCR of both cells treated with the CT and CT-Dex for different time of incubation: 15 min, 30 min, 1 h, 2 h, 4 h and 24 h (data not shown but available from the authors). In Fig. 7, we report the results obtained after 30 min of incubation because this was the most representative time especially for the MIA PaCa-2. In fact in the MIA PaCa-2 we observed a decrease of the VEGF expression level in the cells treated with CT and CT-Dex proportionally to the increased concentration of the CT. However we did not obtain the same result with PL45 cells, in which we did not observe at any time and concentration any significant decrease of the VEGF expression levels. This confirms that PL45 cells are very resistant against the chemotherapeutic drugs, and the high level of the expression of VEGF can be considered one of the features increasing the malignancy of the cells.

CONCLUSION

In this study, we have successfully produced a catechin-dextran conjugate and confirmed the cytotoxicity of this polymeric anticancer drug against pancreatic ductal adenocarcinoma cell lined. The conjugate was synthesized by free

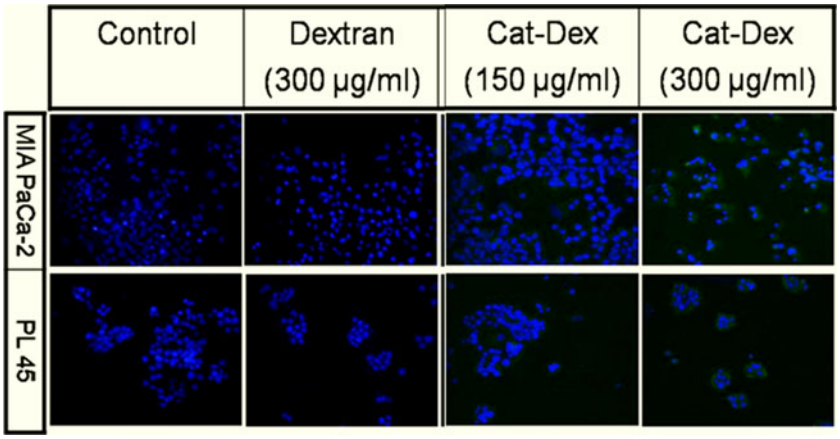

Fig. 6 Evaluation of apoptotic cells after 30 min of incubation dextran-catechin conjugate at 150 μg/ml and 300 μg/ml. These images confirm that both pancreatic tumor cell lines go in apoptosis after incubation with dextran-catechin conjugate. Apoptotic cells are represented by green fluorescent cells. MIA PaCa-2 cells showed 62% of annexin positive cells after 30 min of incubation with catechin-dextran 150 μg/ml, whereas it was observed 73% of positive cells with 300 μg/ml of the conjugate. PL45 tumour cells counted 67% of positive cells with catechin-dextran 150 μg/ml and 85% of green positive cells with catechin-dextran 300 μg/ml.

radical grafting reaction induced by ascorbic acid/hydrogen peroxide redox pair which allows coupling the free radical formed in ortho- and para-positions relative to the hydroxyl group of the flavonoid and the heteroatoms of the polysaccharide without the generation of any toxic reaction products. ^{1}H-NMR, FT-IR and UV-Vis analyses confirmed the chemical incorporation of the flavonoid into the polymeric chain without alteration of the polysaccharide structure as demonstrated by GPC analysis. Folin-Ciocalteu reagent was used to determine the amount of CT bonded per g of conjugate and to assess the increased stability of catechin in the conjugate compared to the free form. The results of the biological tests indicate that the conjugate could be considered for future application in the chemotherapy against pancreatic ductal adenocarcinoma. The MTT assays confirmed significant cytotoxicity against cancer cells, with lower effects on HPNE non neoplastic cells, indicating its potential for reducing systemic cytotoxicity on normal tissues commonly associated with standard chemotherapy regimens. Two different cell lines were studied: MIA PaCa-2 and PL45. Both cell types were dramatically killed (apoptosis) by the conjugate with more efficiency than free CT. However the PCR study showed that, while in the MIA PaCa-2 cells CT and CT-Dex reduced the expression of VEGF, in the PL45 we did not observe any significant difference in the gene expression of VEGF. Future work is envisaged to investigate the effects of CT-Dex conjugate in healthy mice and in a mouse model of pancreatic ductal adenocarcinoma

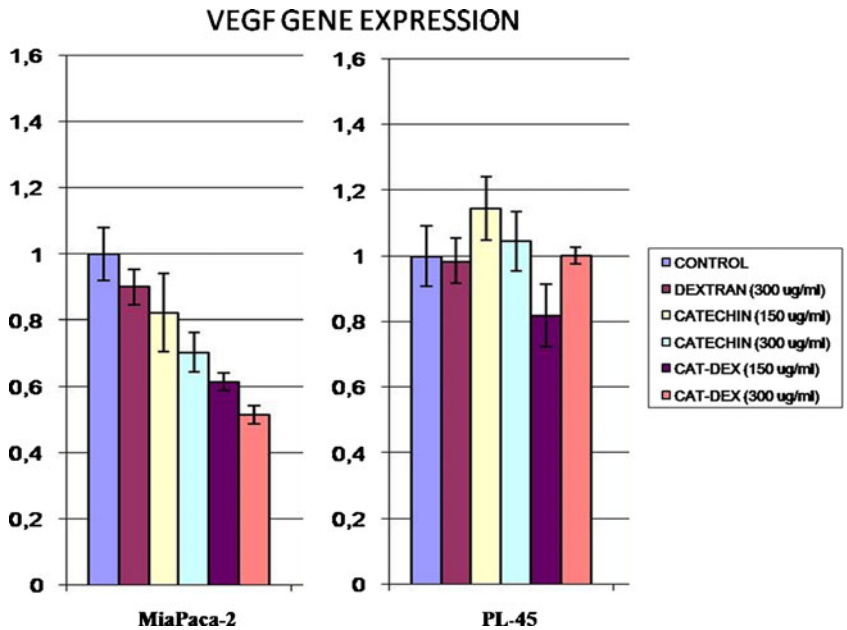

Fig. 7 Quantitative RT-PCR amplification plots of VEGF after 30 min of incubation with the dextran, catechin and dextran-catechin conjugate.

ACKNOWLEDGMENTS & DISCLOSURES

This work was financially supported by MIUR (Programma di ricerca di rilevante interesse nazionale 2008), and University of Calabria funds.

Financial support of Regional Operative Program (ROP) Calabria ESF 2007/2013 – IV Axis Human Capital – Operative Objective M2 - Action D.5 is gratefully acknowledged. Authors are solely responsible for the work.

Authors thank Prof. Alfred Cuschieri from the Medical Science lab Scuola Superiore S. Anna, Pisa, Italy.

REFERENCES

1. Jemal A, Siegel R, Ward E, Murray T, Xu J, Thun MJ. Cancer Statistics, 2007. CA Cancer J Clin. 2007;57:43–66.
2. Baghurst PA, Mc Michael AJ, Slavotinek AH, Baghurst KI, Boyle P, Walker AM. A case–control study of diet and cancer of the pancreas. Am J Epidemiol. 1991;134:167–79.
3. Berrington de Gonzalez A, Sweetland S, Spencer E. A meta-analysis of obesity and the risk of pancreatic cancer. Br J Cancer. 2000;89:519–23.
4. Everhart J, Wright D. Diabetes mellitus as a risk factor for pancreatic cancer: a meta-analysis. JAMA, J Am Med Assoc. 1995;273:1605–9.
5. Li D, Xie K, Wolff R, Abbruzzese JL. Pancreatic cancer. Lancet. 2004;363:1049–57.
6. Burris HA, Moore MJ, Andersen J, Green MR, Rothenberg ML, Modiano MR, *et al.* Improvements in survival and clinical benefit with gemcitabine as first-line therapy for patients with advanced pancreas cancer: a randomized trial. J Clin Oncol. 1997;15:2403–13.
7. Neuhaus P, Oettle H, Post S, Gellert K, Ridwelski K, Schramm H, *et al.* A randomised, prospective, multicenter, phase III trial of adjuvant chemotherapy with gemcitabine *vs*. observation in patients with resected pancreatic cancer. Proc Ann Meet Am Soc Clin Oncol. 2005;4013.
8. Abbruzzese JL. New applications of gemcitabine and future directions in the management of pancreatic cancer. Cancer. 2002;95:941–5.
9. Oettle H, Arning M, Pelzer U, Arnold D, Stroszczynski C, Langrehr J, *et al.* A phase II trial of gemcitabine in combination with 5-fluorouracil (24-hour) and folinic acid in patients with chemonaive advanced pancreatic cancer. Ann Oncol. 2000;11:1267–72.
10. Kurtz J, Kohser F, Negrier S, Trillet Lenoir V, Walter S, Limacher J, *et al.* Gemcitabine and protracted 5-FU for advanced pancreatic cancer. A phase II study. Hepato-Gastroenterology. 2000;47:1450–3.
11. Heinemann V. Gemcitabine: progress in the treatment of pancreatic cancer. Oncology. 2001;60:8–18.
12. Kornek G, Potter R, Selzer E, Schratter A, Pur HU, Rogy M, *et al.* Combined radiochemotherapy of locally advanced unresectable pancreatic adenocarcinoma with mitomycin C plus 24-hour continuous infusional gemcitabine. Int J Radiat Oncol Biol Phys. 2001;49:665–71.
13. Yang CS, Chung JY, Yang G, Chhabra SK, Lee MJ. Tea and tea polyphenols in cancer prevention. J Nutr. 2000;130:472S–8S.
14. Jung YD, Kim MS, Shin BA, Chay KO, Ahn BW, Liu W, *et al.* EGCG, a major component of green tea, inhibits tumour growth by inhibiting VEGF induction in human colon carcinoma cells. Br J Cancer. 2001;84:844–50.
15. Leone M, Zhai D, Sareth S, Kitada S, Reed JC, Pellecchia M. Cancer prevention by tea polyphenols is linked to their direct inhibition of antiapoptotic Bcl-2-family proteins. Cancer Res. 2003;63:8118–21.
16. Pellecchia M, Reed JC. Inhibition of anti-apoptotic Bcl-2 family proteins by natural polyphenols: new avenues for cancer chemoprevention and chemotherapy. Curr Pharm Des. 2004;10:1387–98.
17. Duncan R. Polymer conjugates as anticancer nanomedicines. Nat Rev Cancer. 2006;6:688–701.
18. Vicent MJ, Duncan R. Polymer conjugates: nanosized medicines for treating cancer. Trends Biotechnol. 2006;24:39–47.
19. Greco F, Vicent MJ. Combination therapy: Opportunities and challenges for polymer–drug conjugates as anticancer nanomedicines. Adv Drug Delivery Rev. 2009;61:1203–13.
20. Maeda H. Polymer conjugated macromolecular drugs for tumor-specific targeting. In: Domb AJ, editor. Polymeric site-specific pharmacotherapy. New York: John Wiley and Sons; 1994. p. 95–116.
21. Vasey PA, Kaye SB, Morrison R, Twelves C, Wilson P, Duncan R, *et al.* Phase I clinical and pharmacokinetic study of PK1 [N-(2-hydroxypropyl)methacrylamide copolymer doxorubicin]: first member of a new class of chemotherapeutic agents–drug–polymer conjugates. Cancer Research Campaign Phase I/II Committee. Clin Cancer Res. 1999;5:83–94.
22. Meerum Terwogt JM, Bokkel Huinink WW, Schellens JHM, Schot M, Mandjes I, Zurlo M, *et al.* Phase I clinical and pharmacokinetic study of PNU166945, a novel water soluble polymer conjugated prodrug of paclitaxel. Anti-Cancer Drug Des. 2001;12:315–23.
23. Minko T, Kopeèková P, Pozharov V, Kopeèek J. HPMA copolymer bound Adriamycin overcomes MDR1 gene encoded resistance in a human ovarian carcinoma cell line. J Control Release. 1998;54:223–33.
24. Luo Y, Ziebell MR, Prestwich GD. A hyaluronic acid-taxol antitumor bioconjugate targeted to cancer cells. Biomacromolecules. 2000;1:208–18.
25. Spizzirri UG, Iemma F, Puoci F, Cirillo G, Curcio M, Parisi OI, *et al.* Synthesis of antioxidant polymers by grafting of gallic acid and catechin on gelatin. Biomacromolecules. 2009;10:1923–30.
26. Cirillo G, Puoci F, Iemma F, Curcio M, Parisi OI, Spizzirri UG, *et al.* Starch-quercetin conjugate by radical grafting: synthesis and biological characterization. Pharm Dev Technol. 2009.doi:10.3109/10837450.2010.546413.
27. Cirillo G, Kraemer K, Fuessel S, Puoci F, Curcio M, Spizzirri UG, *et al.* Biological activity of a gallic acid-gelatin conjugate. Biomacromolecules. 2010;11:3309–15.
28. Shrivastava PK, Shrivastava SK. Dextran polysaccharides: successful macromolecular carrier for drug delivery. Int J Pharm Sci. 2009;1:353–68.
29. Garnett MC. Targeted drug conjugates: principles and progress. Adv Drug Delivery Rev. 2001;53:171–216.
30. Cho HJ, Chong S, Chung SJ, Shim CK, Kim DD. Poly-L-arginine and dextran sulfate-based nanocomplex for epidermal growth factor receptor (EGFR) siRNA delivery: its application for head and neck cancer treatment. Pharm Res. 2011. doi:10.1007/s11095-011-0642-z.
31. Shah AN, Summy JM, Zhang J, Park SI, Parikh NU, Gallick GE. Development and characterization of gemcitabine-resistant pancreatic tumor cells. Ann Surg Oncol. 2007;14:3629–37.
32. Itakura J, Ishiwata T, Friess H, Fujii H, Matsumoto Y, Büchler MW, *et al.* Enhanced expression of vascular endothelial growth factor in human pancreatic cancer correlates with local disease progression. Clin Cancer Res. 1997;3:1309–16.
33. Wang H, Helliwell K, You X. Isocratic elution system for the determination of catechins, caffeine and gallic acid in green tea using HPLC. Food Chem. 2000;68:115–21.
34. Pan Y, Zhu J, Wang H, Zhang X, Zhang Y, He C, *et al.* Antioxidant activity of ethanolic extract of Cortex fraxini and use in peanut oil. Food Chem. 2007;103:913–8.

35. Waterman KC, Adami RC, Alsante KM, Hong J, Landis MS, Lombardo F, *et al.* Hydrolysis in pharmaceutical formulations. Pharm Dev Technol. 2002;7:1–32.
36. Lee KM, Nguyen C, Ulrich AB, Pour PM, Ouellette MM. Immortalization with telomerase of the Nestin-positive cells of the human pancreas. Biochem Biophys Res Commun. 2003;301:1038–44.
37. James R, Warburton S. Hemocytometer cell counts and viability studies: cell quantification. In: Doyle A, Grifith JB, editors. Cell and tissue culture: laboratory procedures in biotechnology. London: John Wiley; 1999. p. 57–61.
38. Tomonori N, Keisuke I, Yasuo I. Green tea component, catechin, induces apoptosis of human malignant B cells via production of reactive oxygen species. Clin Cancer Res. 2005;11:6040–9.
39. Diaz G, Liu S, Isola R, Diana A, Falchi AM. Mitochondrial localization of reactive oxygen species by dihydrofluorescein probes. Histochem Cell Biol. 2003;120:319–25.
40. Uyama H, Maruichi N, Tonami H, Kobayashi S. Peroxidase-catalyzed oxidative polymerization of bisphenols. Biomacromolecules. 2002;3:187–93.
41. Quatresooz P, Pierard GE, Pierard-Franchimont C, Arrese JE, Blaise G, Bourguignon R, *et al.* Molecular pathways supporting the proliferation staging of malignant melanoma. Int J Mol Med. 2009;24:295–301.
42. Teo BKK, Goh SH, Kustandi TS, Loh WW, Low HY, Yim EKF. The effect of micro and nanotopography on endocytosis in drug and gene delivery systems. Biomaterials. 2011;32:9866–75.